

EXPERIMENTAL AND NUMERICAL INVESTIGATION OF ADHESIVE BONDING FOR UAVs AND SMALL AIRCRAFTS

Massuda, Andréa Izumi Fukue, andreaif@yahoo.com.br

Bussamra, Flávio Luiz de Silva, flaviobu@ita.br

Hernandes, José Antônio, hernandes@ita.br

ITA - Instituto Tecnológico de Aeronáutica

Divisão de Engenharia Aeronáutica

Praça Marechal Eduardo Gomes, 50 - Vila das Acácias

CEP 12.228-900 – São José dos Campos – SP – Brasil

Abstract. Bonded structures have been widely studied in the last years. Aerospace industries have special interest in bonded joints because they are lighter than mechanical aluminum connections (fastened or riveted). Besides, increase in fatigue life of the structure is expected. For best performance, bonded joints must be submitted to superficial pre-treatment and the adhesive cure must happen under controlled conditions of air humidity and temperature. These procedures are, in general, of prohibitive costs for small aircrafts and UAV's (Unmanned Aerial Vehicles), where simpler preparations are required. In this paper, aluminum bonded joints with different superficial pre-treatments (sanding, spot blasting, chromic acid anodizing, phosphoric acid anodizing), and different cure conditions (24°C, 80°C and 120°C), are submitted to tensile tests and compared. The aim is to compare strengths of joints bonded with different techniques. Also, finite element modeling of bonded joints are presented to predict the strength of the joint, and compared with experimental results.

Keywords: Adhesive bonding, aluminum joint, numerical simulation, UAV – Unmanned Aerial Vehicle

1. INTRODUCTION

The present work investigates the structural bonding for plates with the use of adhesives, and it refers to the superficial pre-treatment, cure temperature, roughness, as well as shear strength by tension loading tests. Besides, finite element modeling is used to predict joints stress distribution. The structure of an aircraft is divided in primary and secondary. Failure of primary structure will result in failure of the component, while failure of the secondary structure will cause local damage. The structural adhesives can be used in both mentioned applications. Bonded structures also might be applied, for example, to UAVs (Unmanned Aerial Vehicles). The application of adhesive in joints (stringers and skin, for example), in place of rivets and welding, would bring reduction of weight, cost and time of maintenance.

In general, prepared surfaces enhance loading capacities. The difference between bonded joints and riveted ones is that in mechanical joints the rivet drills a hole on the adherent to join two parts, creating an orifice in the surface. This discontinuity in the surface causes stress concentration, as shown in Figure 1.

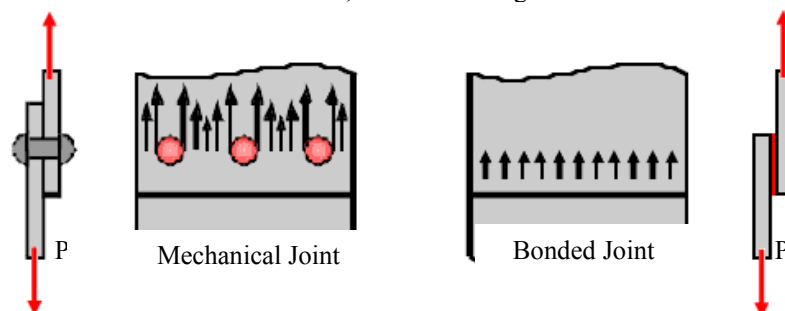


Figure 1. Stress distribution in riveted and bonded joints (Hexel, 1997).

Several factors should be considered when the method of bonded joints is used, including the requirements to take into account in the design such as: purpose of bonding, the most efficient type of adhesive, cost compared with other methods of connection (riveting, welding, etc.), if the bonded structure occasionally must be disassembled for maintenance, service temperature, if the bonded surface should be subjected to superficial pre-treatment, which type of cure (stove or room temperature), and which necessary quality control to guarantee better adhesion.

The bonded joints can bring many benefits. For example, the joints with dissimilar materials with efficient superficial pre-treatments (chromic acid anodizing or CAA and phosphoric acid anodizing or PAA) can be joined and high resistances can be reached if compared with other types of joint as the riveted one.

In the case of joints loaded in tension, the load distribution is basically by shear stress on the adhesive layer. Average shear stress τ_a (Figure 2) is defined by Toolkit, 2002:

$$\tau_a = \frac{P}{L.b} \tag{1}$$

where P is the applied force, L is the overlap length and b is the width.

When a joint is loaded, initially the adhesive has an elastic behavior, but for rigid adhesives under high loads the adhesive is loaded beyond its yield stress in shear circumstances. In addition to that, regions of uniform stress are developed at the edges of the joints as shown Figure 2 (Toolkit, 2002).

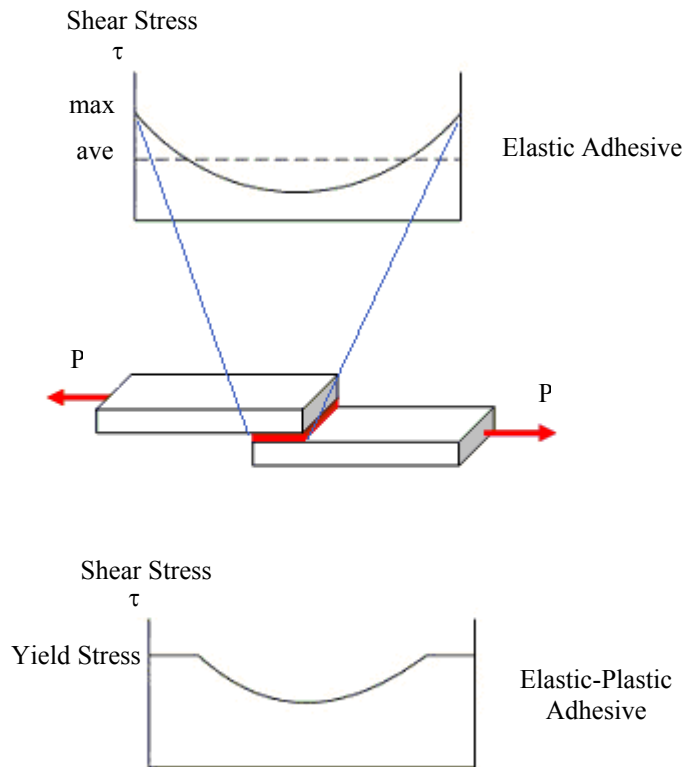


Figure 2. Stress distribution along the joint (Toolkit, 2002)

The joint resistance limit, P_u is given by Toolkit, 2002:

$$P_u = \tau_y . L . b \tag{2}$$

where τ_y is the adhesive shear yielding stress, L is the overlap length and b is the width.

1.1. Superficial Treatments

There are several types of superficial pre-treatments for bonded structures, such as: sanding, spot blasting, chromic acid anodizing (CAA), phosphoric acid anodizing (PAA), etc. In this topic CAA and PAA will be presented.

The CAA process consists of depositing a thick layer of aluminum oxide in the surface. With the addition of a small quantity of chromic acid to the sealing water, an anodizing surface is formed, making the surface adequate for bonding (Wegan, 1989). The process of PAA is done by deposition of aluminum oxide. Physical damages and contamination of the surface of the oxide during the handling of surfaces pre-treated with PAA can present interfacial failure even with low stresses (Wegan, 1989).

1.2. Finite Element Modeling (FEM)

Many approaches using FEM can be applied to adhesive modeling. Tahmasebi (1999) proposed a model using springs and rigid elements, as shown in the Figure 3. This model uses two rigid elements to simulate the thickness of the adhesive (η) that are connected to a plate, and this plate represents the adherent.

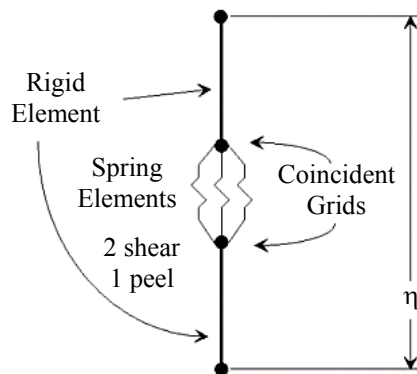


Figure 3. Adhesive modeled as spring and rigid element (Tahmasebi, 1999)

Three spring elements are connected between two rigid elements through two coincident nodes at the centre of the distance between the plates. The spring elements therefore connect the rigid elements. In this model directions of rotations of the springs are considered. Through the elements of plate it is possible to obtain the strength, stresses, energies, etc. Spring elements supply strength and displacements that can be used to determine stresses and energies in the adhesive.

Another model was proposed by Jesus (2003) as shown in Figure 4. The adherent was modeled as an isoparametric shell element (Bathe, 1996 and Cook, 1989), also known as CQUAD4 (John and John, 1994) and the adhesive was modeled as solid elements known as CHEXA8, that has eight nodes and three degrees of freedom for each node (translations u , v and w). The connection between shell element CQUAD4 (adherent) and the solid element CHEXA8 (adhesive) was done through the use of linear equations of restriction, the MPC (Multi Point Constraint).

Several factors are taken into account in the choice of the FEM model. For example, the model with solid elements is simpler to create; so it's more appropriate for big structures. Also, plot stresses can be shown instantly in commercial softwares. In the other hand, spring FEM models demands additional computation in calculation of stresses.

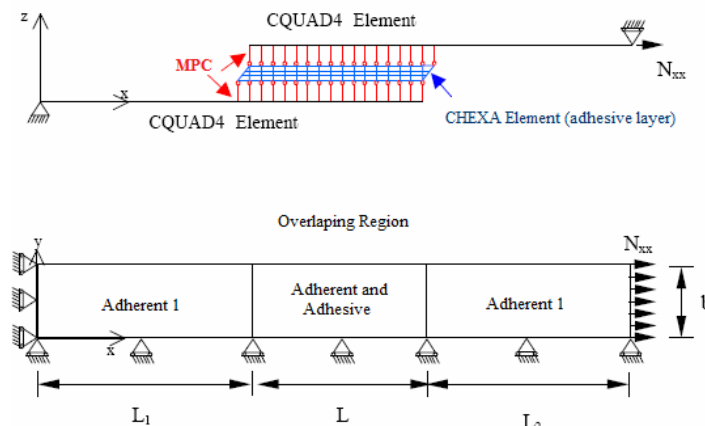


Figure 4. Use of MPC between shell and solid element (Jesus, 2003)

2. EXPERIMENTAL TESTS

2.1. Specimens

Two types of specimens were tested. Specimens' type I was individually cut and machined (ASTM E466). These specimens must be in accordance with Figure 5 after bonded. The specimens' type II was manufactured in multiples of five (ASTM D-1002, 2005). These specimens must agree with the Figure 6 after bonded. The specimens were subjected to the following superficial pre-treatments: sanding, spot blasting, CAA and PAA. Afterwards they were bonded, cured and tested until complete rupture.

For these tests the following materials were used: aluminum 2024-T3, 1.6 mm thickness with Elasticity Modulus $E = 72381$ MPa, Shear Modulus $G = 27574$ MPa and bi-component adhesive (AV. 138) and hardener (HV 998) with $E = 4700$ MPa, $G = 1559$ MPa and allowable shear stress $\tau_a = 13$ MPa and $\tau_a = 16$ MPa for cure temperature of 24°C and 80°C , respectively. The adhesive film AF 163-2K, with supporting carrier, presents the elasticity modulus $E = 1103$ MPa, $G = 429$ MPa and $\tau_a = 29$ MPa.

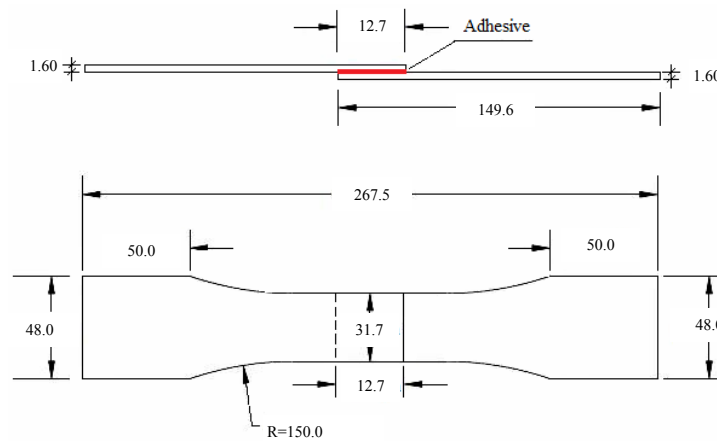


Figure 5. Geometry of notched specimen (mm) – Type I - (after bonding)

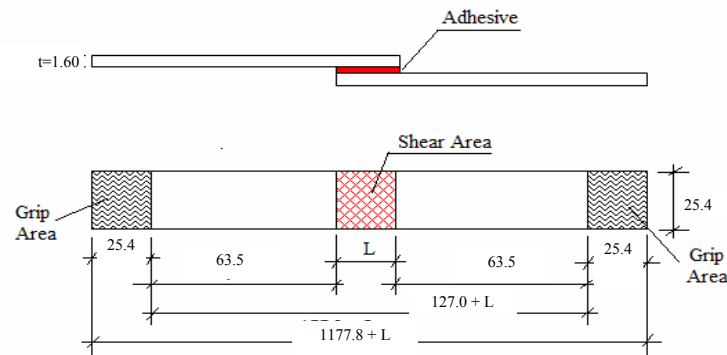


Figure 6. Geometry of flat specimen (mm) – Type II - (after bonding)

The roughness, R_a (Jack, 2001) was measured for each type of superficial pre-treatment. This measure is given by:

$$R_a = \left(\frac{1}{L} \right) \int_0^L h(x) dx \quad (3)$$

where: L is the length passed by the apparatus and $h(x)$ is the deviation of the roughness profile. The middle profile is the line that, in a determined length L , the sum of the areas above the middle profile is the same to the sum of the areas below the profile, considering the surface without waviness. Sixty two (62) specimens were tested in the total.

Table 1 presents the roughness for each treated surface.

Table 1. Roughness R_a for each type of superficial pre-treatment

Specimen Name	Geometry	Pre-Treatment Type					Roughness
		Sanding	Spot Blasting (SB)	CAA	PAA	Sealing (SE)	R_a
Pure Aluminum	notched	x	-	-	-	-	0.26
Sanded Aluminum	notched	x	-	-	-	-	0.36
1	notched	-	-	x	-	-	0.18
2	notched	-	x	x	-	-	2.46
3	notched	-	-	x	-	x	0.15
4	notched	-	x	x	-	x	2.66
5	flat	-	-	-	x	-	0.35

2.2. Shear Strength Test by Tension Loading

The 62 specimens were loaded to the rupture. Figure 7 illustrates the assembly of the test and the broken specimen.

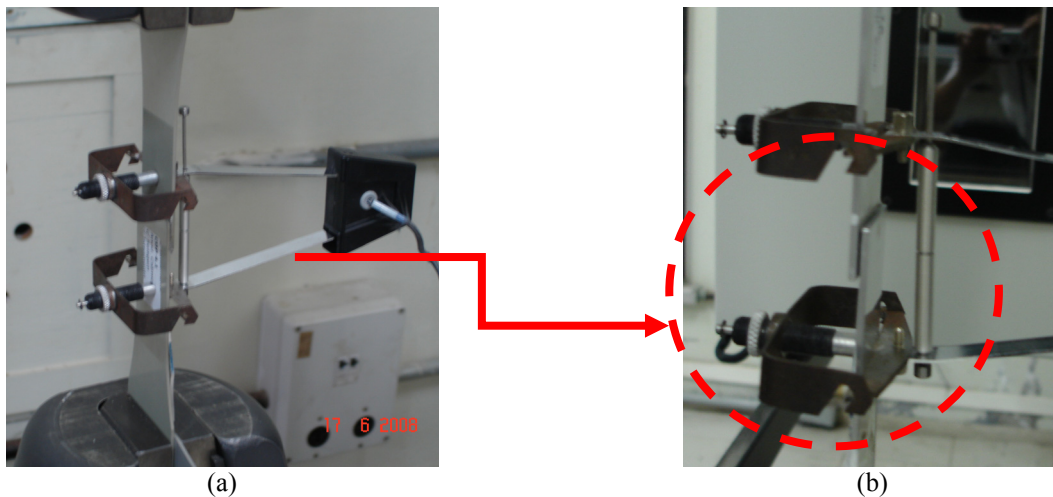


Figure 7. Tension Test: installation of the gauge and broken specimen

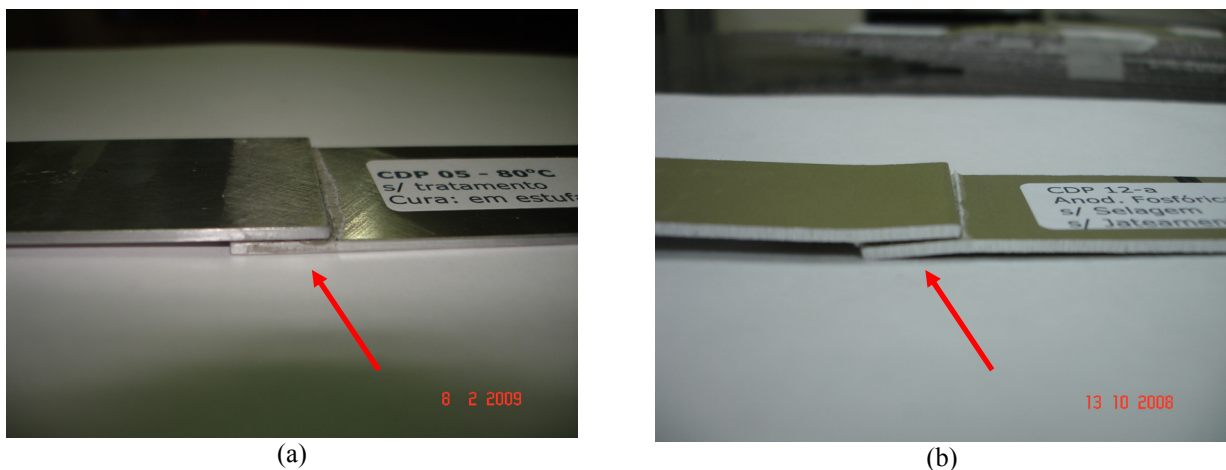


Figure 8. (a) Specimen type I (notched) – elastic bending and (b) Specimen type II (flat) – plastic bending

Different bending patterns are shown in Figure 8. Due to eccentric loading, specimens type I experiments an elastic bending. For the specimens Type II (flat) there is a plastic bending. This deformation is due to the fact that the specimens type I (notched) has bigger width (31.7 mm) if compared with specimen type II width (25.4 mm) .

2.3. Experimental Results

Table 2 shows the strength of the shear test for each type of superficial pre-treatment. F_u , measured in N, is the maximum force applied until the rupture. T_{amb} refers to the cure temperature of 24 °C (room temperature) and T_{80} refers to cure temperature of 80 °C.

Table 2. Test results for each type of specimen

Specimen Name	Geometry	Quantity of Specimen Tested	Pre-Treatment Type						Adhesive Type	Cure Temperature [°C]	F_u [N]	%
			Cleaning	Sanding	Spot Blasting	CAA	PAA	Sealing				
T_{amb}	notched	5	x	x	-	-	-	-	bi-component	24	4478.01	100
T_{80}^o	notched	5	x	x	-	-	-	-	bi-component	80	5017.63	112
1	notched	5	x	-	-	x	-	-	bi-component	80	6088.10	136
2	notched	5	x	-	x	x	-	-	bi-component	80	5611.39	125
3	notched	5	x	-	-	x	-	x	bi-component	80	5991.86	134
4	notched	5	x	-	x	x	-	x	bi-component	80	5461.23	122
5	flat	32	x	-	-	-	x	-	Adhesive Film	120	10821.38	242
TOTAL		62										

It can be notice that with the superficial treatment (specimens 1 to 5), the resistance to the rupture increases if compared with specimens without treatment (T_{amb} and T_{80}). The specimen bonded with the bi-component adhesive which supported the biggest load is the specimen 1 that had its surface treated with CAA only, without spot blasting or sealing. The specimens who did not suffer any chemical treatment, only cleaning and sanding, presented smaller resistances (specimens T_{amb}). By changing the cure temperature, it's possible to increase the resistance. For specimens treated with PAA, the resistance of the adhesive film was much bigger if compared with the specimens without any treatment. Besides, as the adhesive film requires superficial treatment, it brings bigger costs if compared with the bi-component adhesive.

3. FINITE ELEMENT MODEL

Figure 9 and Figure 10 illustrate the FEM used in this work. The adhesive was modeled as a solid element of linear behavior and the adherent with elements of plate, according to the study proposed in section 1.2.

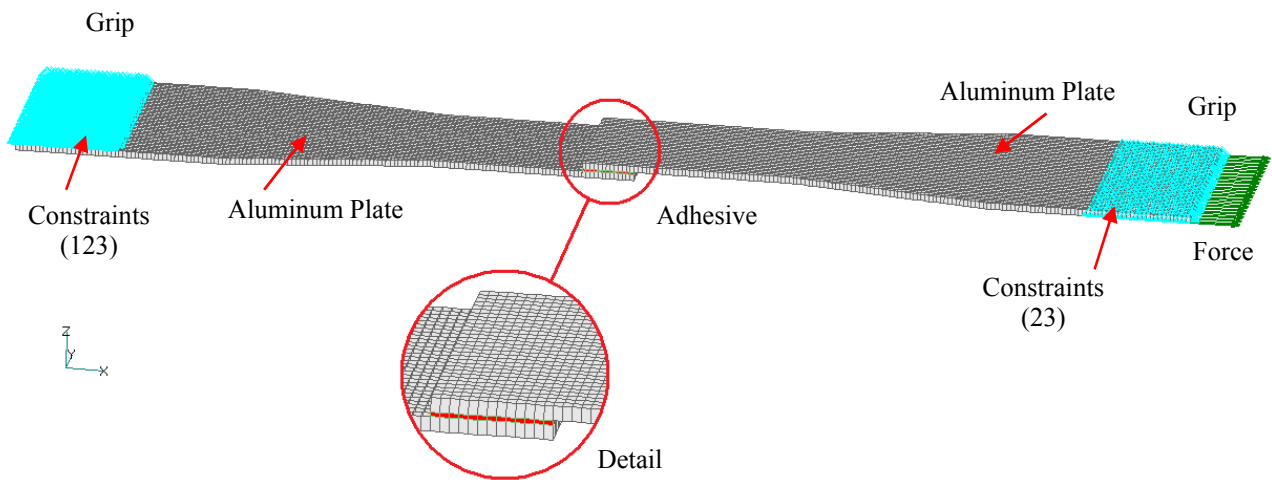


Figure 9. FEM – notched specimen

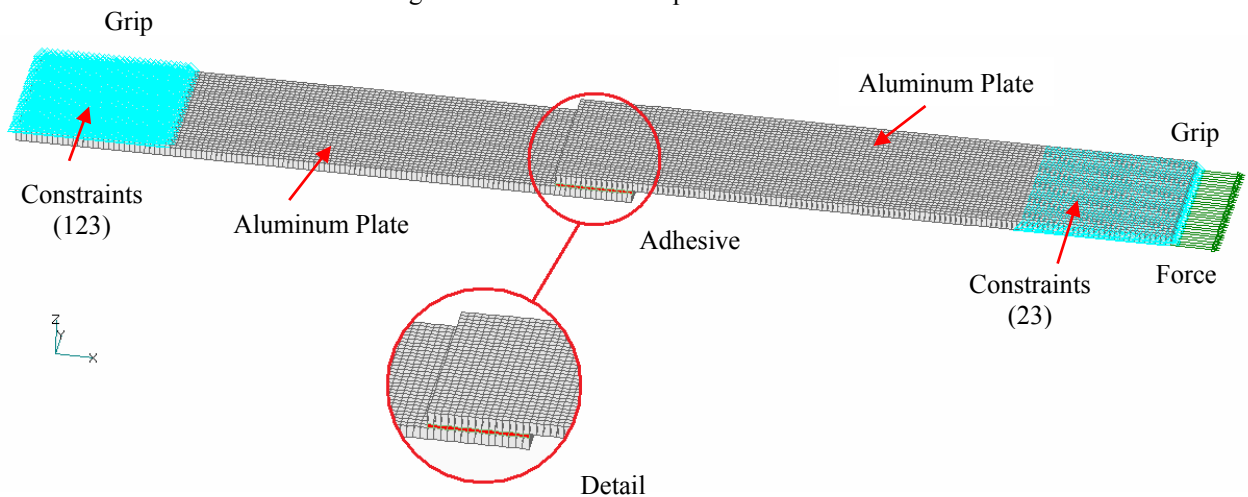


Figure 10. FEM – flat specimen

Mesh details are shown in Figure 11, where NE is the number of solid elements along the width of the specimen.

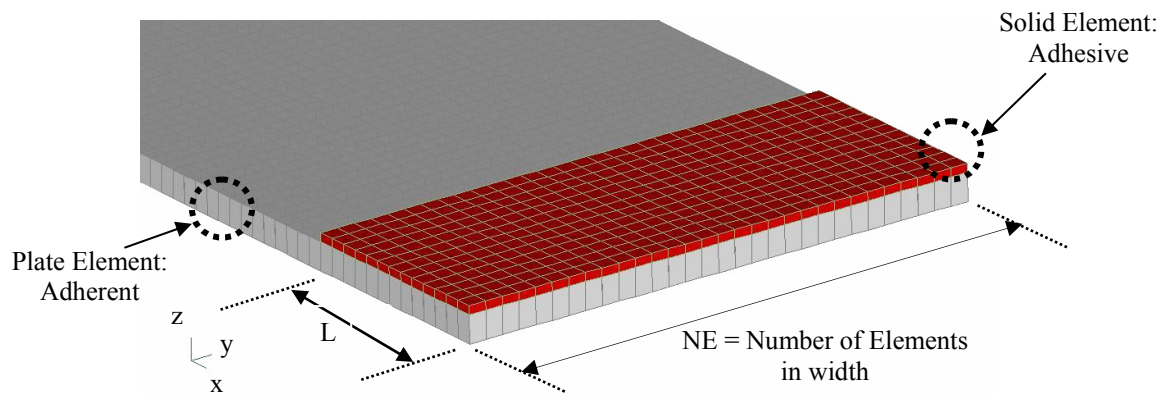


Figure 11. FEM mesh details.

Table 3 presents maximum shear stresses found in five different meshes, when load F_u is applied to the notched specimens, and compares with average shear stress. For $NL=30$, the maximum shear stress is 1.52 times the average stress, as expected (Figure 2).

Table 4 shows the convergence results for flat specimens. It can be noticed that in both cases convergence were found. By increasing NE too much, the model tends to present bad results due bad aspect ratios.

Table 3. Mesh convergence for notched specimens ($t_{adhesive} = 0.50$ mm, adhesive allowable stress= 16 MPa)

Specimen Name	FEM		(NE)	Solid Element Width		Width Average in direction X and Y [mm]	Aspect Ratio	FEM Maximum Shear Stress [MPa]	Experimental Average Shear Stress	
	Nodes	Elements		(X-direction) [mm]	(Y-direction) [mm]				τ_m	[MPa]
MC_10	1800	1578	10	2.54	3.17	2.86	5.71	23.66	15.3	
MC_20	6049	5553	20	1.41	1.59	1.50	3.00	26.4	15.3	
MC_30	12939	12091	30	0.98	1.06	1.02	2.04	27.9	15.3	
MC_40	21114	20834	40	0.75	0.79	0.77	1.54	28.9	15.3	
MC_50	34070	32278	50	0.6	0.63	0.62	1.23	29.6	15.3	

Table 4. NL ($t_{adhesive} = 0.50$ mm, adhesive allowable stress= 29 MPa) – flat geometry

Specimen Name	FEM		(NE)	Solid Element Width		Width Average in direction X and Y [mm]	Aspect Ratio	FEM	TENSILE TEST
	Nodes	Elements		Shear Stress XZ-direction [MPa]	Shear Stress τ_m [MPa]				
MC_10	1034	850	10	2.54	2.54	2.54	5.08	46.60	36.78
MC_20	3864	3400	20	1.27	1.27	1.27	2.54	52.3	36.78
MC_30	8494	7650	30	0.85	0.85	0.85	1.70	54.70	36.78
MC_40	14924	13600	40	0.64	0.64	0.64	1.28	56.10	36.78
MC_50	23154	21250	50	0.51	0.51	0.51	1.02	57.00	36.78

The adhesive in the notched FEM were modeled using the properties of the bi-component adhesive (AV 138+HV 998), while the adhesive in flat FEM were modeled using the properties of the adhesive film (AF-163). It is interesting to notice in Figure 12 that in the middle of the bonding area for the bi-component adhesive, there is almost no stress left. Despite both adhesive have the same behavior, adhesive film can sustain at least 10 MPa of shear stress (Figure 13) in the middle part of the joint.

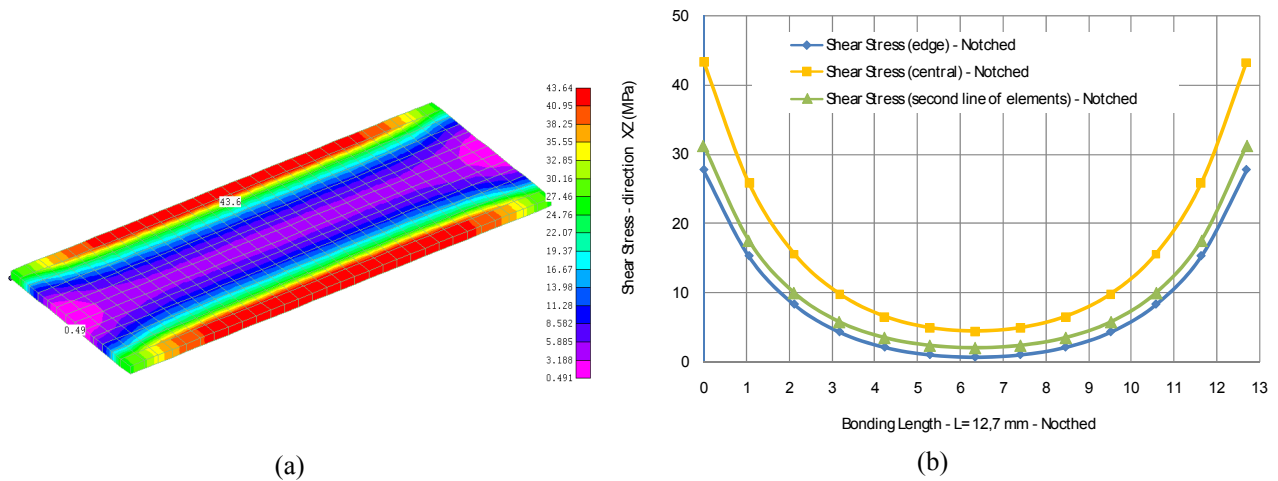


Figure 12. Shear Stress ($F_u= 6106.25$ N – notched FEM): (a) FEM e (b) stress plot

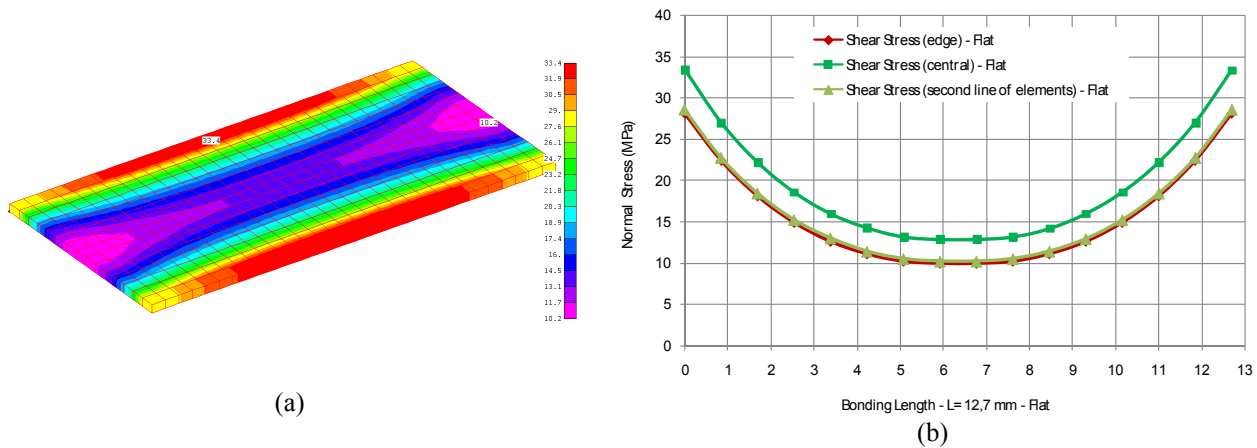


Figure 13. Shear Stress ($F_u= 6106.25$ N – flat FEM): (a) FEM e (b) stress plot

Comparing normal stress between both adhesives, it is possible to notice that they have different behaviors, see Figure 14 (a and b) and Figure 15 (a and b). For the bi-component adhesive, there is no stress at the corner of the joint Figure 14(a-1) and (b-1), blue line, the maximum normal stress occurs at the edge of the joint, Figure 14(a-2) and (b-2) orange line, and then along the joint the stresses are distributed uniformly tending to zero, Figure 14 (a-3), (b-3). In comparison with adhesive film, the normal stress is distributed along the joint not tending to zero. The adhesive film can withstand remaining stress (Figure 15 (b)) in the middle of the joint.

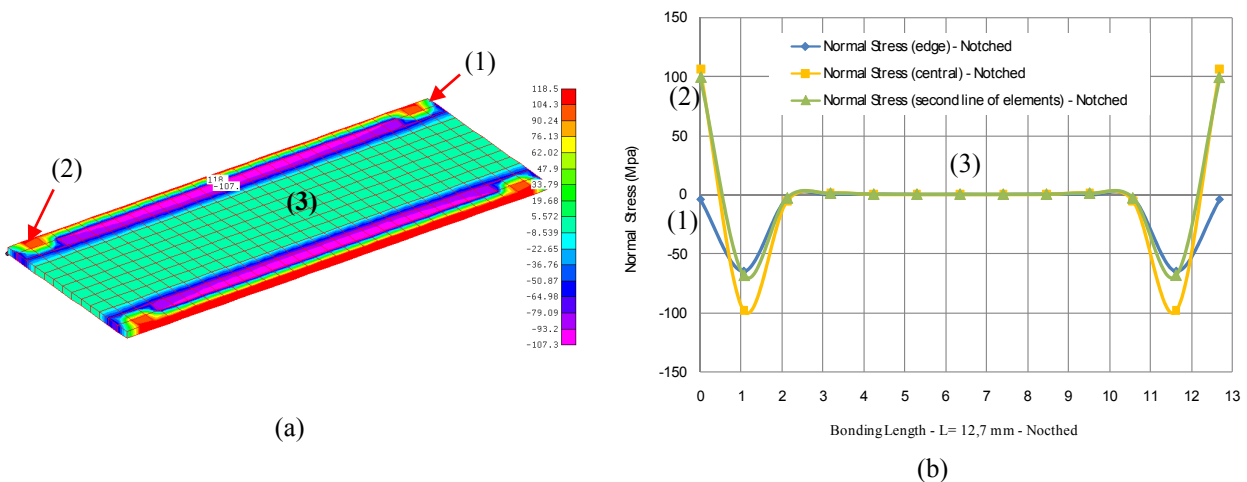


Figure 14. Normal stress ($F_u= 6106.25$ N – notched FEM): (a) FEM e (b) stress distribution

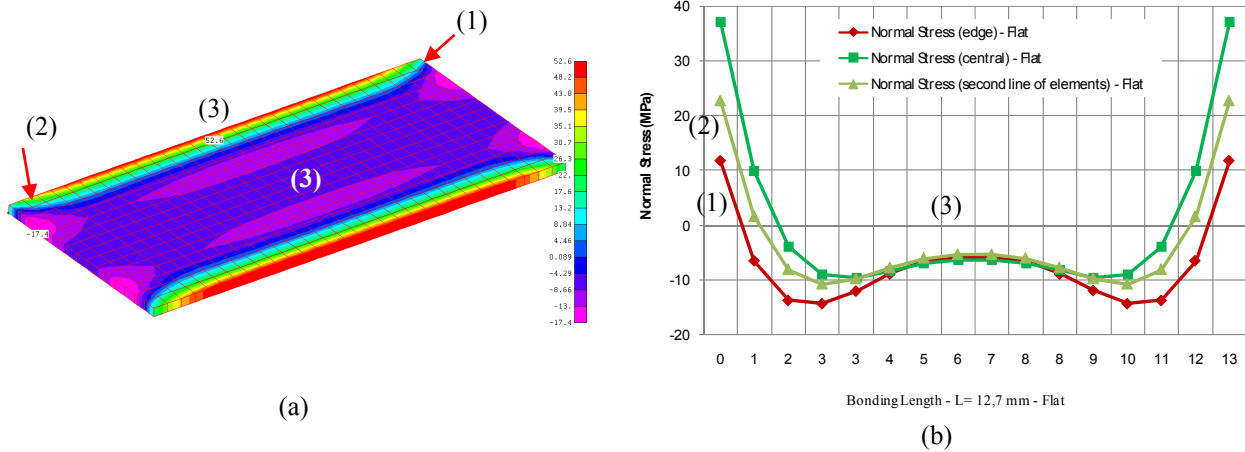


Figure 15. Normal stress ($F_u = 6106.25$ N – flat FEM): (a) FEM e (b) stress distribution

Table 5 shows the FEM comparative results for each surface treatment. FEM models show that Maximum shear stresses (column a) are about 1.8 times the average stress at the failure load (column b). Also, maximum shear stresses are much higher than adhesive allowable stresses, given by manufacturer (column b). In fact, these nominal allowable stresses are comparable with average shear stress. The FEM models were carried out in fully linear analysis.

The correlation (Figure 16) between roughness (R_a) and F_u is -0.35. In general, it shows that high R_a can lead to smaller F_u . This happens because when the surface is spot blasted it can cause damage and/or extraction of material, and then the surface cannot be wet properly and therefore, there is no enough adhesion between adherent and adhesive. High direct correlation (0.95) was found when only sanded, CAA and CAA+SE specimens are taken in account.

Table 5. Comparative results

Specimen Name	Geometry	Quantity of Specimens	F_u [N]	Adhesive Type	Cure Temperature [°C]	(a) FEM Maximum shear Stress [MPa]	(b) Average experimental shear stress [MPa]	(c) Adhesive Allowable Stress [MPa]	a/b (%)
Tamb	notched	5	6106.25	bi-component	24	23.30	12.76	13.00	1.83
80°C	notched	5	6004.60	bi-component	24	22.90	12.55	13.00	1.82
1	notched	5	5573.78	bi-component	80	27.70	15.30	16.00	1.81
2	notched	5	5227.95	bi-component	80	27.20	14.91	16.00	1.82
3	notched	5	5138.70	bi-component	80	25.30	13.84	16.00	1.83
4	notched	5	5052.09	bi-component	80	23.70	12.99	16.00	1.83
5	Flat	32	11865.40	Adhesive Film	120	54.70	36.78	29.00	1.49
TOTAL		62							

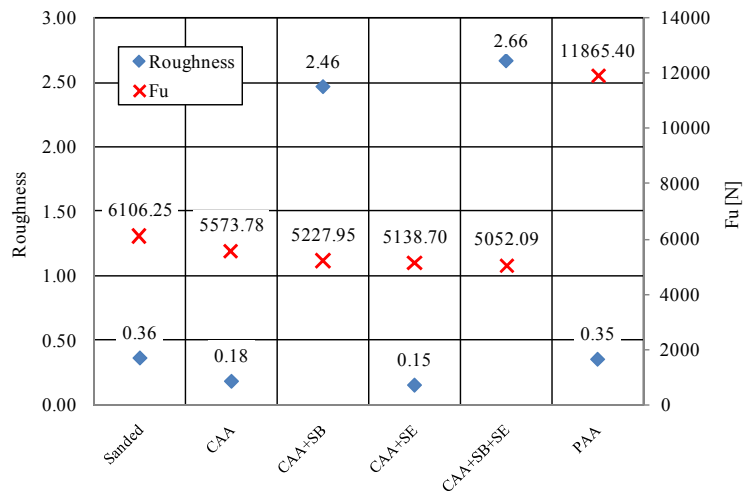


Figure 16. Roughness and F_u

4. CONCLUSIONS

Experimental tests were carried to investigate the influence of superficial pre-treatments in bonded aluminum joints. For bi-component adhesive, the ultimate load vanished from 4478 N (cleaning and sanding only, cure at room temperature) to 5991 N (cleaning and chromic acid anodizing, cure at 80 °C). The former is suitable for low-costs aircrafts, like UAVs and air models, while the latter is suitable for higher budget projects. Adhesive films showed the higher capacity: 10821 N. A cost-benefit analysis must be carried out to determine which method is suitable for one specific project.

The real distribution of stresses, shear stresses in particular, can be predicted with Finite Element models. The FEM modeling presented here was limited to ideal elastic behavior of aluminum and adhesive. Further works must include nonlinearities that occur with high loadings.

5. REFERENCES

- ASTM D-1002, 1 Oct. 2005, "Standard Test Method for Apparent Shear Strength of Single-Lap-Joint Adhesively Bonded Metal Specimens by Tension Loading (Metal-to-Metal)".
- ASTM E466, Jun. 2002, "Standard Practice for Conducting Force Controlled Constant Amplitude Axial Fatigue Tests of Metallic Materials".
- Bath J.K., 1996, "Finite Element Procedures", Ed. Prentice Hall, New Jersey, EUA .
- Cook R.D., Malkus, D.S. and Plesha, M.E., 1989, "Concept and Application of the Finite Element Analysis", Ed. John Wiley, New York, EUA.
- Jack Hugh, 31 Aug. 2001, "Manufacturing Engineering on a disk". 04 May 2009 <<http://www.eod.gvsu.edu/eod/manufact/manufact-79.html>>.
- Tahmasebi F., Jul. 1999, "Finite Element Modeling of an Adhesive in a Bonded Joint", NASA Goddard Space Flight Center.
- Toolkit, 2002. 07 Jul. 2008 <www.adhesivestoolkit.com>
- Wegan R.F., 1989, "Surface Preparation Techniques for Adhesive Bonding", Noyes Publication, Westwood, New Jersey, EUA.

6. RESPONSIBILITY NOTICE

The authors are the only responsible for the printed material included in this paper.